On the accuracy of One-Dimensional Models of Steady Converging/Diverging Open Channel Flows. *

M.E.Hubbard

The University of Reading, Department of Mathematics,

P.O.Box 220, Whiteknights, Reading, Berkshire, RG6 6AX, U.K.

17th February 1999

Abstract

Shallow water flows through open channels with varying breadth are commonly modelled by a system of one-dimensional equations, despite the two-dimensional nature of the geometry and the solution. In this work steady state flows in converging/diverging channels are studied, in order to determine the range of parameters (flow speed and channel breadth) for which the assumption of quasi-one-dimensional flow is valid. This is done by comparing both exact and numerical solutions of the one-dimensional model with numerical solutions of the corresponding two-dimensional flows, and it is shown that even for apparently gentle constrictions, for which the assumptions from which the one-dimensional model is derived are valid, significant differences can occur. Furthermore, it is shown how the nature of the flow depends on the manner in which the boundary conditions are applied by contrasting the solutions obtained from two commonly used approaches.

*This work has been carried out as part of the Oxford/Reading Institute for Computational Fluid Dynamics and was funded by EPSRC.

1 Introduction

For speed and simplicity, one-dimensional models are often used in the modelling of two-dimensional shallow water flows. An example of this is the prediction of the steady flow through an open channel with variable breadth. However, the validity of the one-dimensional model is limited by the assumptions made in its derivation and its accuracy is bound to decrease as the variations in the channel geometry become more severe and the transverse acceleration introduced into the flow gains in significance. Not only are there quantitative differences between the one- and two-dimensional solutions, but the flows obtained may also exhibit major differences in their qualitative features, differing predictions of the existence of hydraulic jumps, for example.

In this work we examine the range of flow parameters (flow speed and size of constriction) for which the one-dimensional model of steady state shallow water flow through a channel of varying breadth accurately represents the full two-dimensional solution. The investigation is used to highlight the limitations of the one-dimensional model as well as to point out those quantities that it is able to predict accurately, especially when the flow exhibits genuinely two-dimensional features and the assumptions underlying the one-dimensional model break down.

Close examination of the mathematical and numerical models also reveals the dramatic effect that changing the form of the boundary conditions can have on the solution, so the results obtained from two commonly-used boundary procedures have been compared in order to illustrate this.

The one- and two-dimensional shallow water models employed are described in Sections 2 and 3 respectively. In one dimension a brief derivation of a family of exact solutions to the equations is also given. The comparison between the two different models is carried out in Section 4 using state of the art numerical techniques to obtain the approximate solutions. This is followed by brief conclusions about the validity of the simpler model.

2 The one-dimensional model

In one dimension, shallow water flow through an open channel of rectangular cross-section and variable breadth can be modelled by the equations

$$\begin{pmatrix} Bd \\ Bdu \end{pmatrix}_t + \begin{pmatrix} Bdu \\ Bdu^2 + \frac{1}{2}gBd^2 \end{pmatrix}_x = \begin{pmatrix} 0 \\ \frac{1}{2}gd^2B_x \end{pmatrix}, \tag{2.1}$$

in which d represents the depth of the flow, u is its velocity, $B = B(x)$ is the variable breadth of the channel and g is the acceleration due to gravity (see, for example [2] for their derivation). Essentially, Equation (2.1) can be derived from the more general, two-dimensional shallow water model under the assumption that $B_x = O(\epsilon)$ for $\epsilon \ll 1$, so that the transverse acceleration of the flow is negligible in comparison with the longitudinal acceleration. In these circumstances the variables d and u are considered to be breadth-averaged quantities. Only steady state solutions are considered in this work, for which the time derivatives are zero. They are only included in (2.1) because they are often used as a numerical device to converge to steady solutions, as is done in the schemes of Section 4 which provide the approximate solutions.

Exact steady state solutions of (2.1) are simple to construct (see for example [7] and related work in which the source terms represent variable bed topography [4, 1]). For a converging/diverging channel with continuously varying breadth the steady solutions of (2.1) can be divided into four categories:

A. continuous - purely subcritical (possibly critical at the most narrow point of the channel, the throat).

B. discontinuous - subcritical at inflow, passing smoothly to supercritical at the throat, then back to subcritical via a stationary hydraulic jump in the diverging region of the channel, remaining so until outflow.

C. continuous - subcritical at inflow, passing smoothly to supercritical at the throat of the channel, and remaining supercritical to outflow.

D. continuous - purely supercritical (possibly critical at the throat).

The particular form taken by the steady solution depends on the boundary conditions which are applied at the entrance and the exit of the channel section being modelled.

The simplest cases are A and D. Integration of the steady equations leads straightforwardly to two quantities which remain constant throughout the channel. These are the total discharge

$$Q \;=\; Bdu\,, \tag{2.2}$$

and the total head

$$H_{\mathrm{T}} \;=\; \frac{u^2}{2g} + d \;=\; \frac{Q^2}{2gB^2d^2} + d\,. \tag{2.3}$$

Given that values for Q and H_{T} can be deduced from the boundary conditions, combining (2.2) with (2.3) leads to

$$d^3 - H_{\mathrm{T}}d^2 + \frac{Q^2}{2gB^2{H_{\mathrm{T}}}^3} \;=\; 0\,, \tag{2.4}$$

an algebraic equation relating the depth of the flow d to the local channel breadth B. This has a pair of physically admissible (positive) solutions for d, one representing subcritical flow and the other supercritical flow, on condition that

$$\frac{B}{B_{\mathrm{in}}} \;\geq\; F_{\mathrm{in}}\left(\frac{3}{F_{\mathrm{in}}^2+2}\right)^{\frac{3}{2}} \tag{2.5}$$

for all values of B in the given channel geometry, where $F_{\mathrm{in}} = u_{\mathrm{in}}/\sqrt{gd_{\mathrm{in}}}$ is the local Froude number specified at inflow. The solution which is chosen by the equations (2.1) depends on the boundary conditions applied (unless both Q and H_{T} are specified, in which case the choice remains open).

When equality holds in (2.5) for some value of B within the channel geometry the flow becomes critical for the values of Q and H_{T} implied by the boundary conditions. However, any critical point of the flow must lie at the throat of the channel so, unless equality is satisfied there, the inlet values of Q and/or H_{T} change automatically to satisfy the boundary condition at inflow *and* the critical condition at the throat ($F = 1$ when $B = B_{\mathrm{min}}$). The flow is then of type B or C. Furthermore, the variation of the Froude number upstream of the critical point in such situations is uniquely defined, being the subcritical solution ($0 < F < 1$) of the equation

$$F^2\left(\frac{3}{F^2+2}\right)^3 \;=\; \left(\frac{B_{\mathrm{min}}}{B}\right)^2\,. \tag{2.6}$$

This implies that the Froude number at inflow is fixed by the channel geometry, taking the same value whenever the solution is transcritical (so F is not a practical choice for specification as an inflow boundary condition). The new values of Q and $H_{\rm T}$ for the smooth region of the flow which surrounds the critical point can be calculated by combining the subcritical inflow boundary condition with this inflow Froude number.

Downstream of the critical point, the flow type (B or C) is determined by the outflow boundary conditions. Initially, since the flow is continuous through the critical point, the solution retains the upstream values of Q and $H_{\rm T}$ but switches to the supercritical branch of (2.4) downstream of the throat. If no jump occurs the supercritical solution values found using (2.4) are retained throughout the rest of the channel.

When a stationary hydraulic jump occurs (which must always be from supercritical flow to subcritical flow), equations (2.1) lead to two quantities which are continuous across the jump. These are given by

$$[du] \;=\; 0 \qquad \text{and} \qquad \left[du^2 + \frac{1}{2}gd^2\right] \;=\; 0\,. \tag{2.7}$$

The first of these, together with (2.2), implies that Q is constant throughout the domain for any steady flow, but from the second and (2.3) it is clear that there is a jump in $H_{\rm T}$ when the flow is discontinuous. Thus the flow downstream of a stationary hydraulic jump is determined by the value of Q which has been calculated for the transcritical upstream flow and the boundary condition specified at outflow.

Combining the two expressions (2.7) leads to a relationship between the branches of the solution on either side of the jump, given by

$$d_+ \;=\; \frac{d_-}{2}\left(\sqrt{1 + 8{F_-}^2} - 1\right)\,, \tag{2.8}$$

in which d_+ is the depth immediately downstream of a discontinuity, while d_- and F_- are the depth and local Froude number immediately upstream. The flow sustains a stationary hydraulic jump if

$$(d_+)_{\rm out} \;\le\; d_{\rm out} \;\le\; d_{\rm in} \tag{2.9}$$

where $(d_+)_{\text{out}}$ is calculated using (2.8) together with the assumption that the jump occurs at the furthest downstream point of the constriction. Given the boundary conditions and the critical condition, (which imply the values of Q and H_{T} the solution on either side of the discontinuity can be calculated from (2.4), so it remains to find the point within the constriction at which condition (2.8) is satisfied. Both the upstream and downstream values of total head (H_{T_-} and H_{T_+} respectively) are known, and the upstream Froude number at the jump (F_-) can be found by solving iteratively the equation

$$16(H_{\text{T}_-} - H_{\text{T}_+})\left(\sqrt{1+8{F_-}^2}-1\right) - \frac{2H_{\text{T}_-}}{{F_-}^2+2}\left(\sqrt{1+8{F_-}^2}-3\right)^3 = 0\,, \quad (2.10)$$

which can be deduced from the jump conditions (2.7). The position of the jump is then found by combining (2.10) with (2.6).

One important point to note here is the effect which the choice of boundary condition has on the solution. In numerical calculations a wide variety of conditions are applied, two of the most commonly used forms being

1. Q specified at subcritical inflow, d at subcritical outflow.

2. R^+ specified at subcritical inflow, R^- at subcritical outflow, where $R^\pm = u \pm 2\sqrt{gd}$ are the Riemann invariants of the homogeneous system.

At a supercritical inflow boundary all solution variables are specified, while nothing is specified at supercritical outflow.

Figure 2.1 illustrates the type of solution obtained using both sets of boundary conditions. Note its close resemblance to Figure 3 of [4] which was constructed in a similar manner for channel flows with variable bed topography instead of variable breadth. The flow parameters which have been specified are B_{min}, the minimum breadth of the channel (the shape of the channel need not be specified yet), and F_{in}, the 'initial' Froude number of the flow (the inflow Froude number proposed before any adjustments are made to Q and H_{T} due to the onset of transcritical flow). The latter, along with the condition that the 'initial' depth is given by $d_{\text{in}} = 1.0$, determine the values of the variables chosen to be prescribed at inflow and outflow boundaries (and also the initial conditions required by

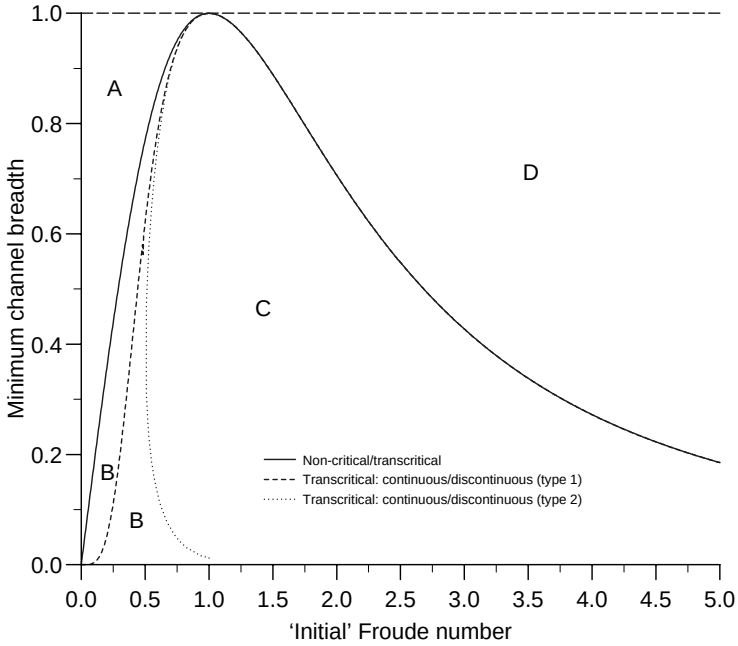

Figure 2.1: Types of exact solution to constricted channel flow test cases given different boundary conditions.

the numerical schemes in Section 4). The solid line in the figure indicates the transition between smooth flow, type A or D, and transcritical flow, type B or C, the broken/dotted lines represent the transition from discontinuous type B flow to smooth type C flow. Note that for supercritical 'initial' Froude numbers these three curves coincide.

When F_{in} is subcritical the transition to transcritical flow is independent of the type of boundary conditions applied but, particularly for the more severe channel constrictions, it is noticeable that type 2 boundary conditions are far more likely to sustain discontinuous flow. This difference in behaviour may well be due to the inhomogeneous nature of the equations (2.1), and the consequence that the Riemann invariants are not constant along characteristics. This suggests that type 1 boundary conditions should be used, simply to facilitate comparison with experiment where Q and d are both measurable. The solutions depicted in Figure 2.2 confirm this. Although there is little difference to be seen between the depth profiles when $B_{\text{min}} = 0.9$, the more extreme case shows very little resemblance between the solutions. Even though one would not expect an accurate prediction by the one-dimensional model for such a narrow constriction, this still suggests

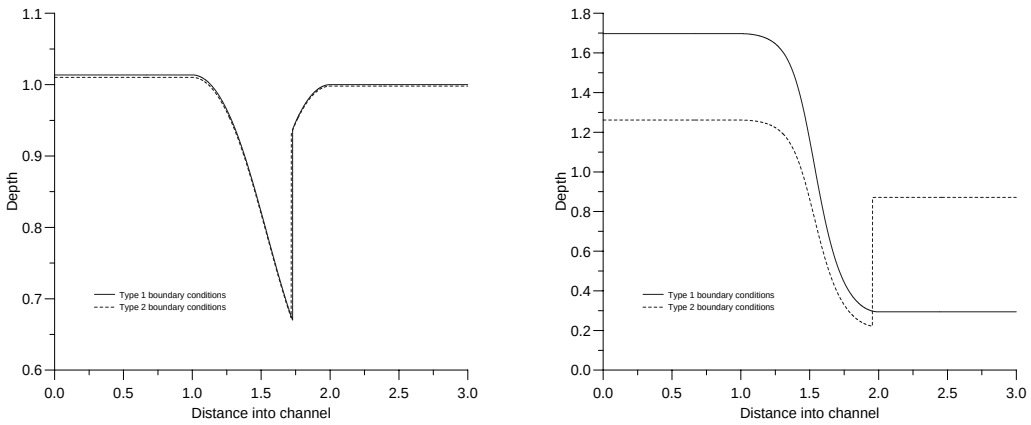

Figure 2.2: Exact solutions for different boundary conditions: $B_{\min} = 0.9$, $F_{\text{in}} = 0.67$ (left); $B_{\min} = 0.4$, $F_{\text{in}} = 0.5$ (right).

that type 1 boundary conditions should be used.

3 The two-dimensional model

In two dimensions, the shallow water equations are given in conservative form by

$$\underline{\mathbf{U}}_t + \underline{\mathbf{F}}_x + \underline{\mathbf{G}}_y = \underline{\mathbf{0}}\,, \tag{3.1}$$

where

$$\underline{\mathbf{U}} = \begin{pmatrix} d \\ du \\ dv \end{pmatrix}, \quad \underline{\mathbf{F}} = \begin{pmatrix} du \\ du^2 + \frac{1}{2}gd^2 \\ duv \end{pmatrix}, \quad \underline{\mathbf{G}} = \begin{pmatrix} dv \\ duv \\ dv^2 + \frac{1}{2}gd^2 \end{pmatrix}, \tag{3.2}$$

in which d is the depth of the flow, u and v are the x- and y-velocities of the flow respectively, and g is the acceleration due to gravity. The effects of the varying breadth of the channel are applied solely by the shape of the domain over which these equations are solved and the boundary conditions which are applied so, unlike the one-dimensional model, these equations have no source terms.

4 Numerical results

The one-dimensional numerical scheme used in this work combines Roe's approximate Riemann solver [11], as applied to the shallow water equations (2.1) [10], with the minmod limiter [12] within a MUSCL algorithm [13], together with a recently developed upwind discretisation of the source term [6]. In two dimensions, the discretisation used is the multidimensional upwind method of Mesaros and Roe [3, 8], applied to the shallow water equations, (3.1) and (3.2), on unstructured triangular grids [5].

For the purposes of this comparison, each of the results presented is for a channel of length 3 units which has a symmetric constriction of length 1 unit at its centre whose breadth is given by

$$B(x) \;=\; \begin{cases} 1.0 - (1.0 - B_{\min})\cos^2(\pi(x - 1.5)) & \text{for} \quad |x - 1.5| \;\leq\; 0.5 \\ 1.0 & \text{otherwise}\,, \end{cases} \tag{4.1}$$

where $B_{\min}$ is the minimum channel breadth and x is the distance into the channel (so the throat is positioned at the midpoint of the constriction). In the two-dimensional case the constriction has been chosen for simplicity to be represented by symmetric indentations on either side of the channel (as illustrated in Figure 4.6). Whilst alternative constructions undoubtedly alter the flow in some way, their effect on the comparison with one-dimensional results is not significant.

Each of the one-dimensional numerical solutions is obtained on a uniform 76 node grid, giving comparable resolution to the two-dimensional grids used, each of which has been constructed using a simple advancing front technique (see for example [9]) with an underlying mesh spacing parameter of 0.04. The initial conditions for each numerical experiment (in which the steady state solution is achieved by approximating the evolution of the time-dependent shallow water equations (2.1) with steady boundary conditions and converging to the steady state from the initial conditions as $t \to \infty$) were $d = 1.0$ and $F = F_{\text{in}}$, with $v = 0.0$ in two dimensions.

Figure 4.1 shows how well the one-dimensional numerical results agree with the theory (as illustrated in Figure 2.1) in terms of the parameter values ($B_{\min}$

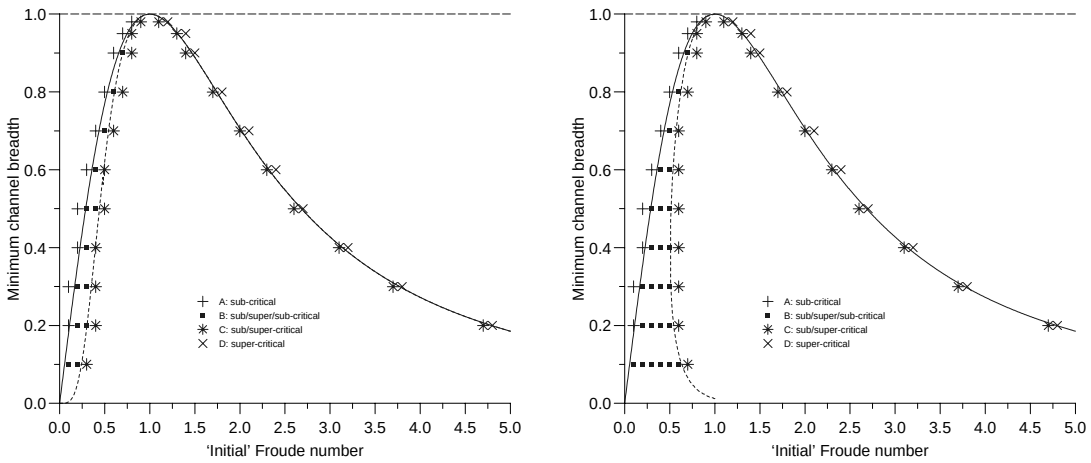

Figure 4.1: Types of one-dimensional numerical solution to constricted channel flow test cases with boundary conditions of type 1 (left) and type 2 (right).

and F_{in}) at which transition occurs between the different types of steady solution obtained. Different symbols have been used to indicate the types of solution (A-D) predicted by the numerical scheme. Regions of the graph have been left empty, but the solution type is implied by the symbol on the boundary of the region. (Note that with the more commonly used approximations to the source terms, such as a simple pointwise evaluation, the agreement with theory is less close. In some cases they can predict unphysical phenomena, such as a continuous steady state which is supercritical at both inflow and outflow but has a subcritical region around the throat of the channel.)

The corresponding two-dimensional numerical results are shown in Figure 4.2. In this case, type 1 boundary conditions correspond to specifying du and setting $v = 0$ at subcritical inflow and d at subcritical outflow; type 2 boundary conditions being where $R^+ = u + 2\sqrt{gd}$ and $v = 0$ are specified at subcritical inflow and $R^- = u - 2\sqrt{gd}$ is given at subcritical outflow (where it has been assumed that these boundaries are parallel to the y-axis). It is immediately clear that the multidimensional nature of the geometry has a significant effect on the solution, the differences occurring whenever the two-dimensional flow is not smooth. This includes every steady state which has some supercritical component (*cf.* Figure 4.6). As expected, the more narrow the constriction the greater the effect, but even the smallest indentation allows a steady state solution which is supercritical

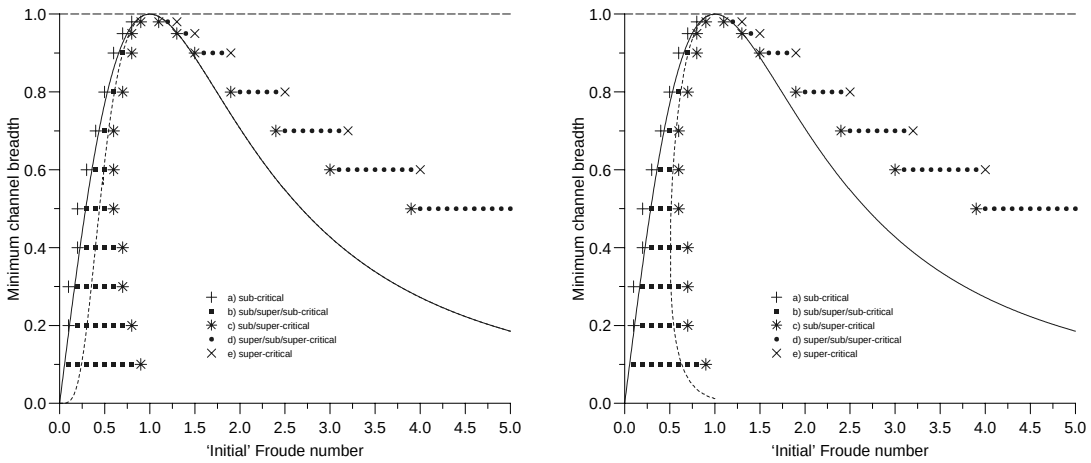

Figure 4.2: Types of two-dimensional numerical solution to constricted channel flow test cases with boundary conditions of type 1 (left) and type 2 (right).

at both inflow and outflow but has a subcritical pocket within the constriction.

In two dimensions there are five different types of solution which may occur:

a) Smooth and purely subcritical.

b) Subcritical at inflow and outflow, critical at the channel throat, with a steady discontinuity in the diverging region of the channel.

c) Smooth (apart from the oblique jumps in two dimensions), subcritical at inflow, critical at the throat, and supercritical at outflow.

d) Smooth in one dimension, supercritical at inflow and outflow, with oblique jumps and a subcritical region in the constriction for two-dimensional flow.

e) Smooth in one dimension and purely supercritical in every case.

This corresponds to the one-dimensional situation, with the addition that case D of Section 2 has now split into two cases, d) and e).

Interestingly, the type of solution generated in two dimensions no longer depends to any great extent on the type of boundary condition which has been employed. (There is only one difference between the two graphs of the numerical results in Figure 4.2, at $B_{\min} = 0.2$, $F_{\text{in}} = 0.7$.) This close resemblance may well be due to the fact that, unlike the one-dimensional system, the two-dimensional equations are homogeneous. Quantitatively though, there is still a

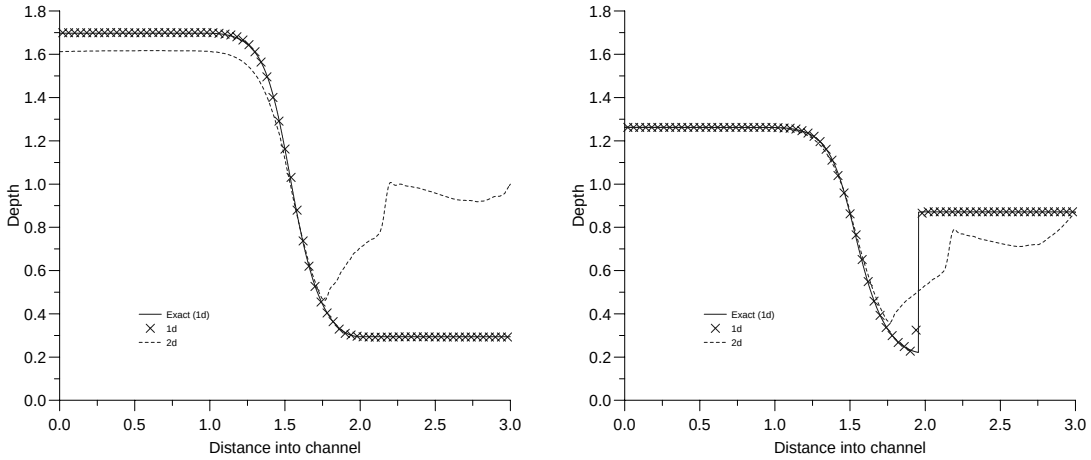

Figure 4.3: Comparison of depth for $B_{\min} = 0.4$ and $F_{\text{in}} = 0.5$ with boundary conditions of type 1 (left) and type 2 (right).

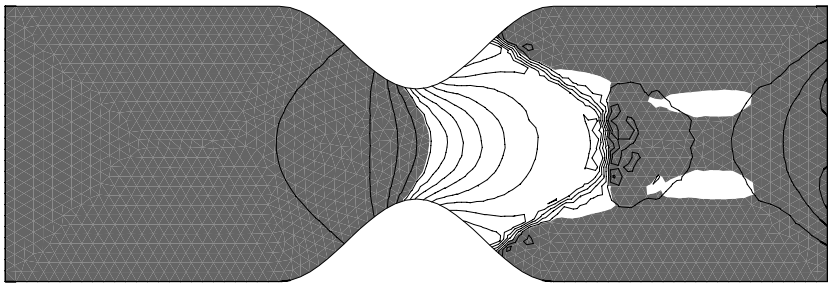

Figure 4.4: Depth contours for $B_{\min} = 0.4$ and $F_{\text{in}} = 0.5$.

considerable difference between the corresponding steady state solutions, particularly in the more extreme cases. This is illustrated in Figure 4.3 in which analytical and numerical solutions to the one-dimensional equations are compared with breadth-averaged numerical solution values obtained in two dimensions. The depth contours shown in Figure 4.4 for type 2 boundary conditions illustrate the two-dimensional nature of the highly curved hydraulic jump in this case.

For type 1 boundary conditions there is also a noticeable difference at inflow between the one- and two-dimensional solutions. The agreement becomes closer at the upstream boundary as the channel is extended away from the constriction, suggesting that the assumption which has been made that the flow is uniform along the whole of each subcritical inflow and subcritical outflow boundary is invalid. The advantages of using type 1 boundary conditions are retained from one

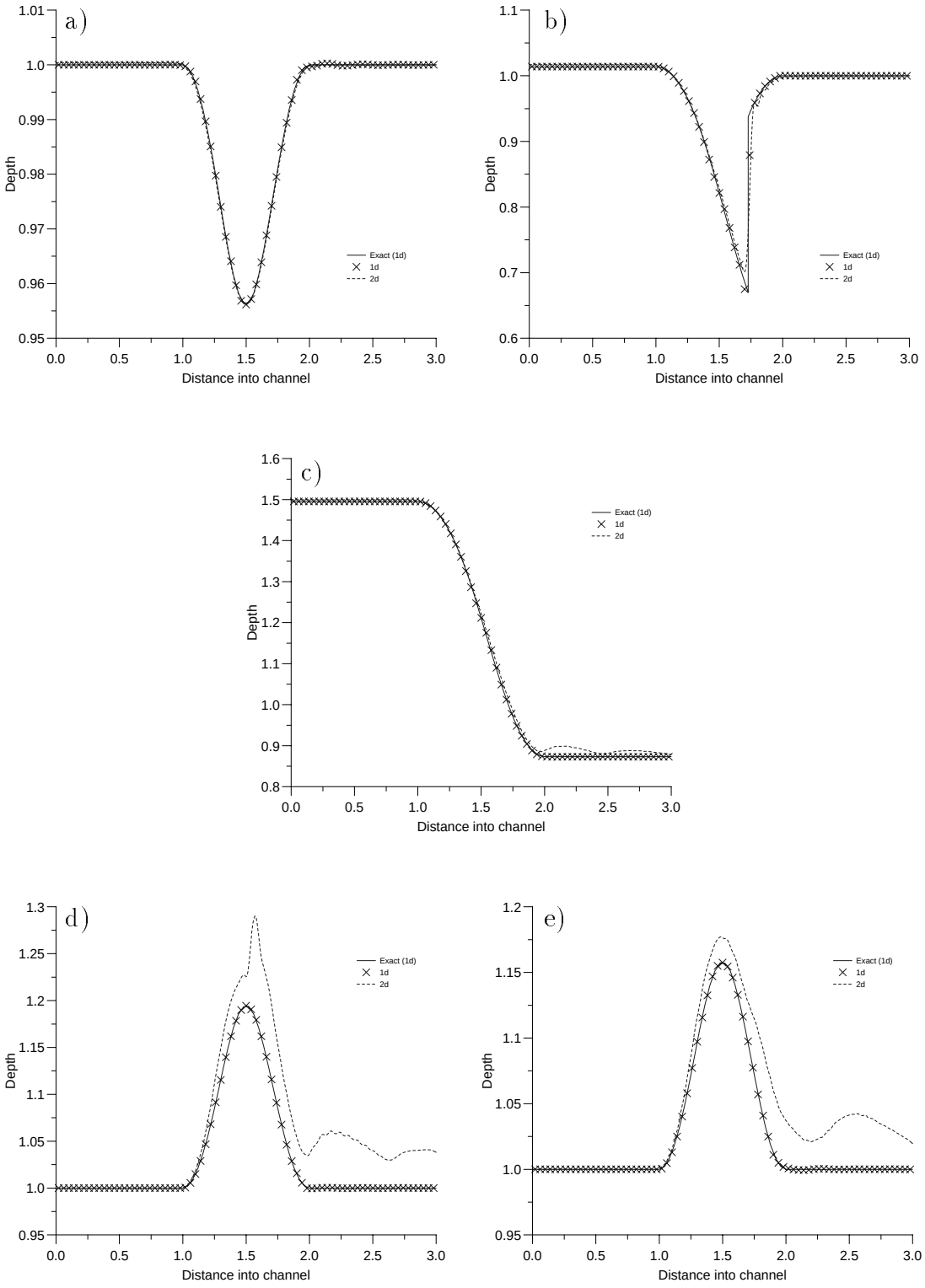

Figure 4.5: Comparison of depth for $B_{\min} = 0.9$ with initial Froude numbers F_{in} of a) 0.5, b) 0.67, c) 1.2, d) 1.7 and e) 2.0.

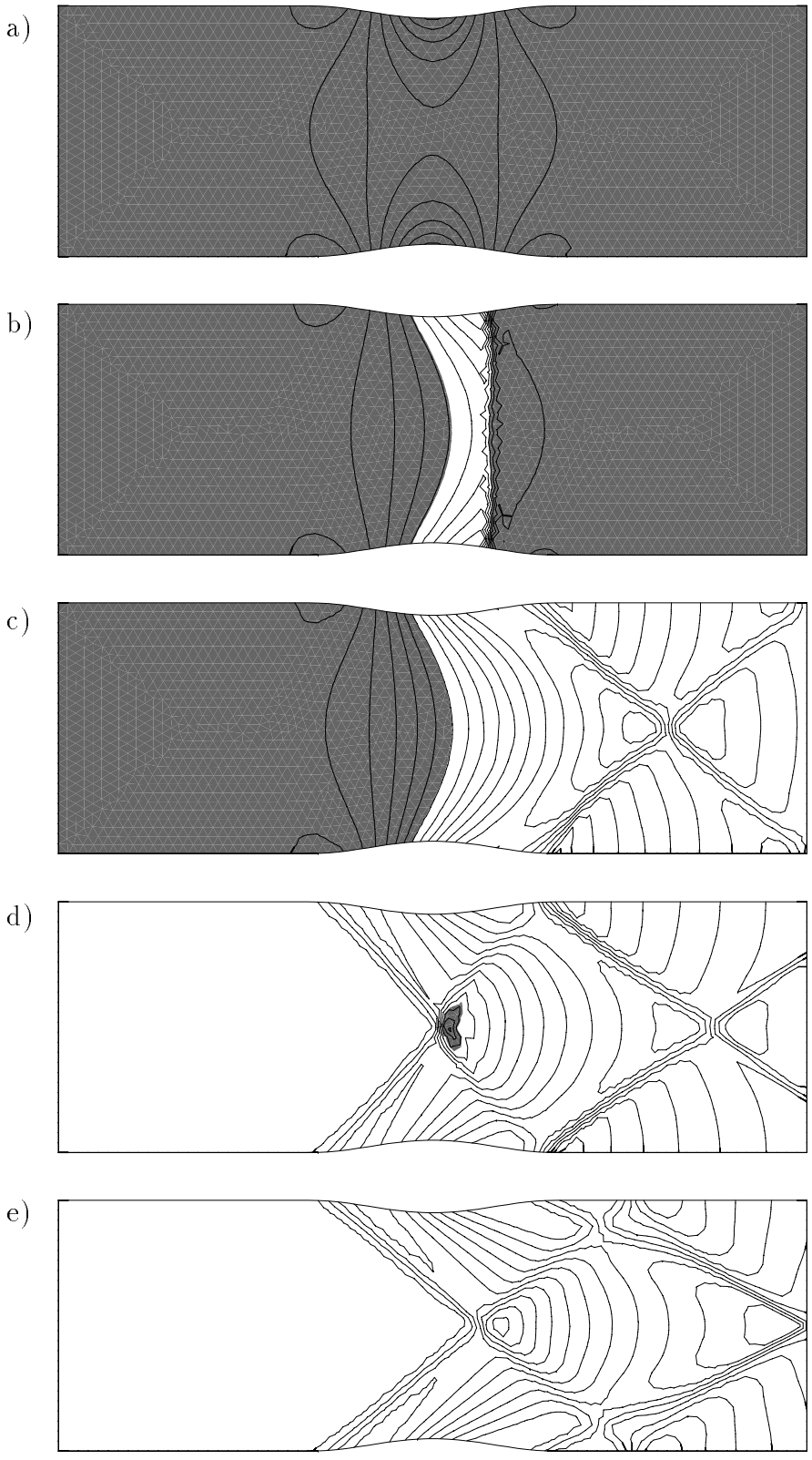

Figure 4.6: Depth contours for $B_{\min} = 0.9$ with initial Froude numbers F_{in} of a) 0.5, b) 0.67, c) 1.2, d) 1.7 and e) 2.0.

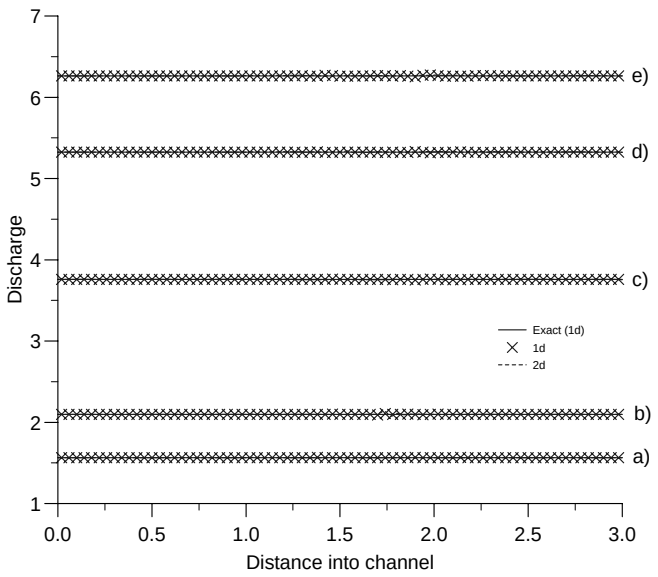

Figure 4.7: Comparison of discharge for $B_{\min} = 0.9$ with initial Froude numbers F_{in} of a) 0.5, b) 0.67, c) 1.2, d) 1.7 and e) 2.0.

dimension, but there is a stronger argument for using type 2 boundary conditions in two dimensions since they are considerably more robust when the transverse variation of the solution is not accounted for at the boundary.

Figure 4.5 shows each of the five different types of solution obtained for a less extreme channel geometry using type 1 boundary conditions. The corresponding contour plots of depth for the two-dimensional solutions are shown in Figure 4.6 (subcritical regions have been shaded to distinguish them). In order to illustrate the conservative nature of the numerical schemes, profiles of discharge Q along the channel are plotted in Figure 4.7. Except for some small perturbations close to discontinuities the numerical schemes maintain the correct constant value of Q throughout the channel in each case. The discrepancies which can be seen between the one-dimensional exact and numerical results (which are in close agreement) and the two-dimensional breadth-averaged results at the higher Froude numbers can be clearly related to the appearance of oblique discontinuities (undular jumps) triggered by the constriction when the flow becomes supercritical at outflow. The influence of the oblique discontinuities on supercritical flow is illustrated even more dramatically in Figures 4.8 and 4.9, which depict the depth of the flow for a

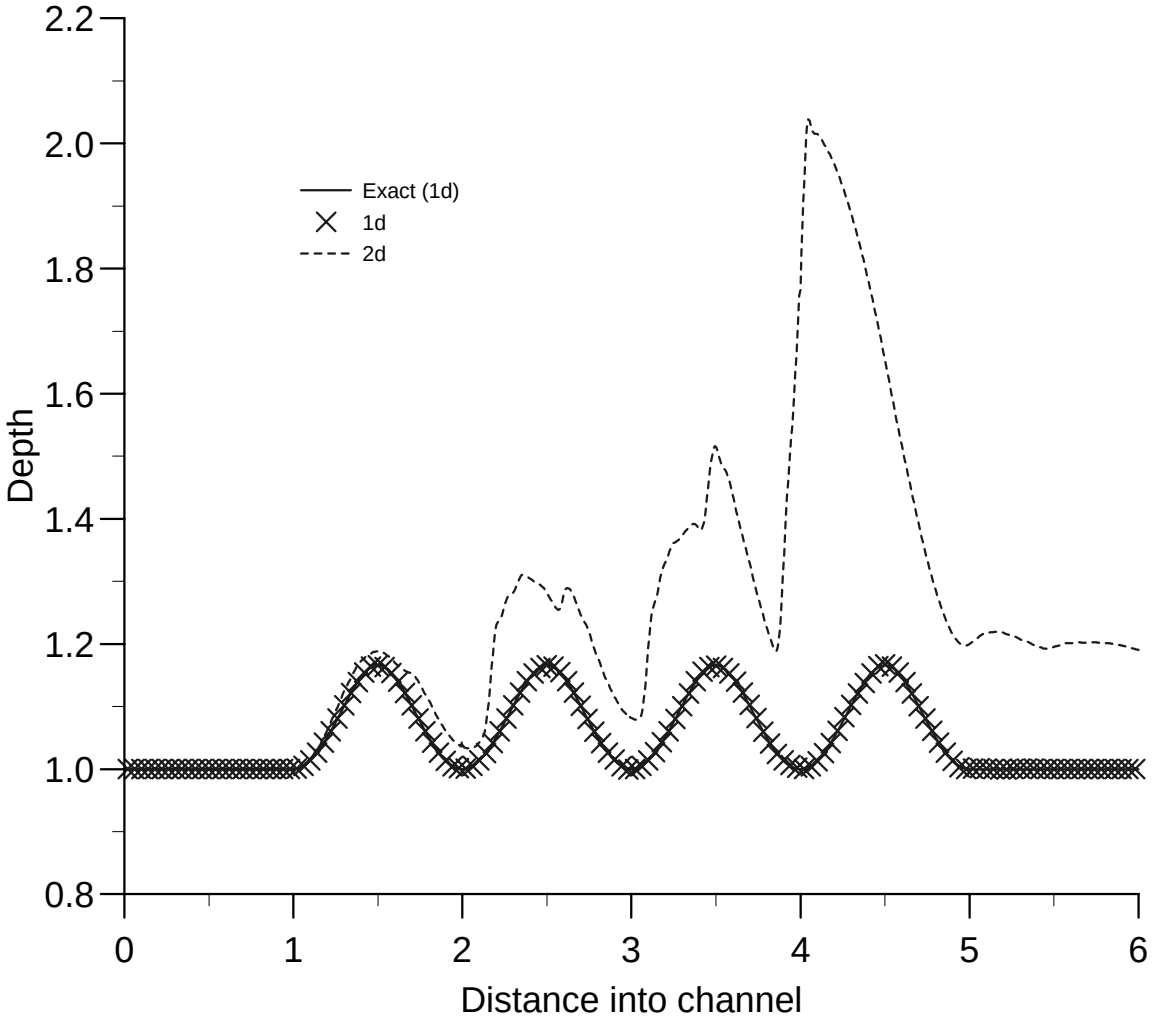

Figure 4.8: Comparison of depth for the quadruple constriction test case with $B_{\min} = 0.9$ and $F_{\text{in}} = 1.9$.

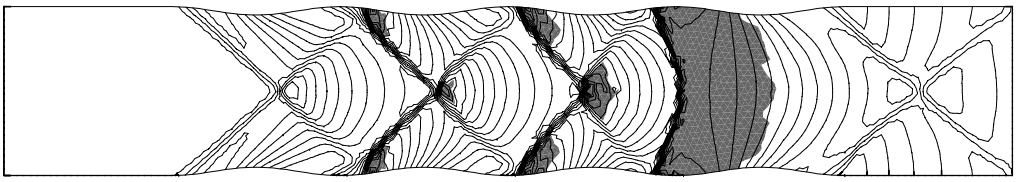

Figure 4.9: Depth contours for the quadruple constriction test case with $B_{\min} = 0.9$ and $F_{\text{in}} = 1.9$.

channel with a quadruple symmetric constriction with $B_{\min} = 0.9$ and $F_{\text{in}} = 1.9$. The one-dimensional model predicts smooth supercritical flow throughout, but the comparison with two dimensions becomes progressively worse as the jumps interact with each other.

5 Conclusions

In this work a comparison has been made between one- and two-dimensional models of steady state shallow water flow through an open channel of varying breadth. It has been shown that the numerical and analytical solutions to the one-dimensional model agree closely, provided that an appropriate discretisation of the source terms is employed.

When the flow is completely smooth and subcritical these solutions also prove to be an accurate prediction of the breadth-averaged two-dimensional flow. For small constrictions ($B_x \ll 1$) the agreement remains good even when the one-dimensional model predicts a discontinuous flow, because the transverse acceleration in the flow is negligible and consequently the two-dimensional solution remains essentially one-dimensional. As the constriction narrows, however, steady hydraulic jumps become more curved and the one-dimensional model less accurate. When the flow downstream of the constriction is supercritical, the undular jumps which are propagated from the constriction in the two-dimensional case cannot be predicted by the one-dimensional equations and the accuracy of the simpler model is poor, even for channels with relatively small indentations which should satisfy the assumptions under which the one-dimensional model is derived. The agreement does however become closer again as the speed of the flow increases and these discontinuities become aligned with the channel.

Two commonly used forms of boundary condition have been compared, and it has been shown that when the flow is transcritical they can give widely differing solutions for given geometries and initial flow parameters. In one dimension specifying discharge at inflow and depth at outflow seems appropriate, since both their values can be determined simply from experiment. In two dimensions however, when the equations are homogeneous, specifying Riemann invariants proves

to be more robust.

Acknowledgements

The author would like to thank Dr. D. Porter and Prof. M. J. Baines for their contributions to this work, Dr. I. MacDonald for the use of his one-dimensional code, and the EPSRC for providing the funding for the author.

References

[1] A.S.Broad, D.Porter and M.J.Sewell, 'New shallow flows over an obstacle', *Q. J. Mech. Appl. Math.*, **50**(4):625–653, 1997.

[2] J.A.Cunge, F.M.Holly and A.Verwey, *Practical aspects of computational river hydraulics*, Pitman, 1980.

[3] H.Deconinck, R.Struijs, G.Bourgois and P.L.Roe, 'High resolution shock capturing cell vertex advection schemes for unstructured grids', *Computational Fluid Dynamics*, number 1994–05 in VKI Lecture Series, 1994.

[4] D.D.Houghton and A.Kasahara, 'Nonlinear shallow fluid flow over an isolated ridge', *Comm. Pure Appl. Math.*, **21**:1–23, 1968.

[5] M.E.Hubbard and M.J.Baines, 'Conservative multidimensional upwinding for the steady two-dimensional shallow water equations', *J. Comp. Phys.*, **138**:419–448, 1997.

[6] M.E.Hubbard and P.Garcia-Navarro, 'Flux difference splitting and the balancing of source terms and flux gradients', in preparation.

[7] I.MacDonald, M.J.Baines, N.K.Nichols and P.G.Samuels, 'Steady open channel test problems with analytic solutions' Numerical Analysis Report 3/95, Department of Mathematics, University of Reading, 1995.

[8] L.M.Mesaros and P.L.Roe, 'Multidimensional fluctuation schemes based on decomposition methods', AIAA Paper 95–1699, 1995.

[9] J.Peraire, M.Vahdati, K.Morgan and O.C.Zienkiewicz, 'Adaptive remeshing for compressible flow computations', *J. Comput. Phys.*, **72**:449–466, 1987.

[10] A.Priestley, 'Roe-type schemes for super-critical flows in rivers', Numerical Analysis Report 13/89, Department of Mathematics, University of Reading, 1989.

[11] P.L.Roe, 'Approximate Riemann solvers, parameter vectors, and difference schemes', *J. Comput. Phys.*, **43(2)**:357–372, 1981.

[12] P.K.Sweby, 'High resolution schemes using flux limiters for hyperbolic conservation laws', *SIAM J. Numer. Anal.*, **21**:995–1011, 1984.

[13] B.van Leer, 'Towards the ultimate conservative difference scheme V. A second order sequel to Godunov's method', *J. Comput. Phys.*, **32**:101–136, 1979.